



Experimental and Computational Study of Thiophene Based Calamitic Liquid Crystals

MARTALA VENKATESWARA REDDY^{1,6}, BATHINI VEERAPRAKASH³, B. MAHESH⁵,
MALA RAMANJANEYULU^{2,4} and P. VENKATESWARLU^{1*}

¹Department of Chemistry, Sri Venkateswara University, Tirupati, India.

²Organic and Bio-organic Chemistry Laboratory, CSIR-Central Leather Research Institute, Adyar, Chennai, India.

³Polymer Science & Technology Laboratory, CSIR-Central Leather Research Institute, Adyar, Chennai, India.

⁴Academy of Scientific and Innovative Research (AcSIR), Ghaziabad, India.

⁵Government College for Men(A), Kadapa, Andhra Pradesh, India.

⁶PSC & KVSC Government Degree College, Nandyala, Andhra Pradesh, India.

*Corresponding author E-mail: profvenkateswarlu05@gmail.com

<http://dx.doi.org/10.13005/ojc/390117>

(Received: October 26, 2022; Accepted: January 04, 2023)

ABSTRACT

The structurally analogous calamitic mesogens 4-((4-(decyloxy) phenoxy) carbonyl) phenyl thiophene-2-carboxylate [2TWC10] and 4-(Thiophen-3-yl) phenyl 4-dodecylbenzoate [S12] based on thiophene were synthesized and structures of the molecules were confirmed by spectroscopic techniques. Among the two molecules, only 2TWC10 mesogen with alkoxy terminal exhibited a typical threaded structure indicating a homeotropic nematic phase under hot stage-polarizing optical microscopy (HOPM). Further, it is supported by differential scanning calorimetry (DSC). Remarkably, alkyl terminal S12 mesogen is not showing liquid crystalline properties. This is because S12 has alkyl group as the terminal group instead of alkoxy group which was used generally, resulting in bent shape to the molecule which reduced aspect ratio which is essential for liquid crystalline property. UV-Visible absorption maxima because of π - π^* transitions in these mesogens were found at 280-300nm in chloroform solution. The DFT study shows that the alkoxy terminal in 2TW10 is contributing to polarity of the molecule but in S12 there is no contribution from terminal chain because it is non polar group. The DFT study also shows that 2TWC10 is more reactive and less stable than S12 molecule.

Keywords: Nematic phase, Photo-physical, Thiophene, DFT Study, Calamitic.

INTRODUCTION

Heterocyclic thiophene based liquid-crystalline materials found potential use in optical information storage, photovoltaic cells, organic

thin-film transistors, spatial light-modulation, fast switching ferroelectric materials, in optical signal processing, fluorescent probes, chemosensors and so on¹⁻³. The extent of use of liquid crystalline molecules in various fields depends on molecular



structure and their organization because structure and organization influence their properties⁴. So, the properties of these molecules are dependent on substituents, hetero cyclic rings and π -conjugated cores. The conjugation in the core is responsible for charge carrier mobility in the liquid crystal molecules. The thiophene based π -functionalized mesogen with imine and ester-based moieties exhibit fluorescence in addition to liquid crystalline property, so these moieties have been used for inducing light responsive and optical properties in the molecules⁵⁻¹⁰. Due to this, thiophene unit was extensively used in the design of topologically different mesogens such as discotic, bent-core, polycatenar, dendron, star-branched, V-shape, cone type, ring form and polyphilic molecules¹¹⁻¹⁴. The trend of insertion of thiophene ring in the core of mesogen gained significance as it reduces the melting point and viscosity, increases optical anisotropy and induces negative dielectric anisotropy. It also alters the symmetry of micro or nano segregation, molecular shape as well as mesophase formation¹⁵⁻¹⁶. The functionalized thiophene liquid crystalline oligomers and polymeric thiophenes are used in plastics, electronics, organic photovoltaic, solid-state lasers, field-effect transistors, radio frequency identification tags, and sensors¹⁷⁻²⁰. These promising materials exhibit a high charge transporting organic semiconductors of the ordered alignment of molecules²⁰⁻²². It is also found that self-organization by the liquid crystalline molecule is one of the critical approaches to controlling the order and packing with an aim to suppress the defect formation usually found in non-mesogenic organic materials²³⁻²⁸.

In the present work, thiophene based three ring compounds were synthesized. 2TWC10 and S12 were chosen to understand the effect of terminal chain and direct bond between thiophene and phenyl ring in core on liquid crystalline property. The structures of the molecules were confirmed using spectroscopic techniques. The phase behaviour and mesomorphism of the thiophene compounds were investigated using the HOPM and their enthalpies were measured using DSC. The absorption maxima of the compounds were measured with UV-Visible absorption spectroscopy. The structure and property relationship was investigated. The energy minimized model structures and dipole-moment of two mesogens were obtained from density functional theory (DFT).

EXPERIMENTAL

Materials

4-dodecylbenzoic acid, 4-hydroxy benzaldehyde, 4-bromophenol and 2-thiophene carboxylic acid were purchased from Sigma-Aldrich Chemicals & Co India. N, N -dimethylformamide, thionyl chloride (SOCl_2), ethanol, Triethylamine, tetrahydrofuran and methanol were bought from SD Fine, Mumbai. n-hexane, hydrochloric acid, n-heptane, Silica gel (100-200 mesh), ethyl acetate, acetone, isopropanol, potassium bromide, ethyl methyl ketone (EMK), acetonitrile, dichloromethane, anhydrous sodium sulphate, calcium chloride, sodium hydroxide, and sodium bicarbonate were purchased from AVARA chemicals (India).

Measurements

An ABB BOMEM MB3000 was used for measuring FT-IR spectroscopy. The JEOL ECA 500NMR spectrometer was used for measuring ^1H and ^{13}C NMR spectra. The Carl Zeiss Axiocam MRC5 polarizing microscope attached with Linkam THMS 600 stage was used for identifying phases and transition temperatures. The A2M digital camera imager was used to capture the texture of mesophase. DSC Q200 TA instruments Q-10 series was used for conducting Differential scanning calorimetry (DSC). The data collected from second heating and cooling cycle was used for the study after conducting two heating and cooling cycles for each sample²⁹. The Becke's three-parameter hybrid exchange functional and Lee-Yang-Parr correlation functional (B3LYP) method employing 6-31G(d) basis set. Gaussian 03W suite of program was used for density functional theory (DFT) calculations³⁰⁻³². Shimadzu UV-1800 spectrophotometer was used for obtaining absorption spectra in solution.

Synthesis

The synthetic route of thiophene based mesogens are shown in Schemes 1-2. 4-((4-(decyloxy)phenoxy)carbonyl)phenylthiophene-2-carboxylate (2TWC10) was prepared by esterification using respective carboxylic acids coupled with 4-decyl oxy phenol using DCC/DMAP method and 4-(thiophen-3-yl)phenyl 4-dodecylbenzoate (S12) prepared by Suzuki method.

Synthesis of 4-formylphenyl thiophene-2-carboxylate [I]

To 4-hydroxy benzaldehyde (5.0 g, 40 mmol) dissolved in ethyl methyl ketone, Triethylamine (3.3 mL, 23 mmol) dissolved in same solvent was added slowly. To the reaction mixture 2-thiophene carbonyl chloride (5.9 g, 40 mmol) was added slowly at 0°C through dropping funnel and it was stirred for 4 hours. Then, the precipitated triethyl ammonium chloride salt was removed by filtration and filtrate was evaporated. The obtained solid was recrystallized from hot isopropyl alcohol.

Yield: 88%, colourless solid, m.p.: 89-91°C, FT-IR: 3102 (aromatic C-H stretching), 2813, 2721, 2064 (C-H), 1721 (C=O), 1603, 1592 (aromatic C=C stretching), 1409, 1356, 1304 (C-H_{bending}), 1261, 1206, 1153 (C-O-C of ester and ether). ¹H NMR (500 MHz, CDCl₃): 9.90 (d, *J*=2.1, 1H), 7.99 (d, *J*=4.0, 1H), 7.93 (d, *J*=8.6, 2H), 7.69 (t, *J*=5.5 1H), 7.39 (d, *J*=8.5, 2H), 7.18 (m, 1H). ¹³C NMR (125 MHz, CDCl₃): 191.03, 159.92, 155.33, 135.33, 134.30, 134.18, 132.20, 131.35, 128.33 and 122.53.

Synthesis of 4-((thiophene-2-carbonyl) oxy) benzoic acid [II]

4-formyl phenyl thiophene-2-carboxylate (1.0 g, 4.3 mmol) was dissolved in tetrahydrofuran (THF) placed in flask. A mixture of anhydrous sodium dihydrogen phosphate (NaH₂PO₄) (4.7 g, 4 mol) and sodium chlorite (NaClO₂) (8 g, 4 mol) dissolved in 25 mL distilled water and slowly added to the flask at 0°C using dropping funnel³³. The reaction was stirred for 10 hours. After completion of reaction the solution was neutralized with 10% sodium bicarbonate (NaHCO₃) solution to get white solid precipitate. The obtained solid was recrystallized from hot n-heptane. Yield 78%, colourless solid powder. FT-IR (KBr, cm⁻¹): 3074 (C-H of aromatic ring), 2932, 2864.9 (C-H of alkyl chain), 2662, 2549 (O-H of -COOH) 1734 (C=O ester), 1682 (C=O of -COOH), 1603 and 1528 (C=C), 1478, 1427 (C-H bending), 1252, 1206 and 1164 (C-O-C of ester and ether groups). ¹H NMR (500 MHz, DMSO-d₆) δ 8.0 (d, *J*=8.6, 2H), 7.9 (d, *J*=3.7 1H), 7.7 (dd, *J*=4.9, 1.0, 1H), 7.2 (d, *J*=8.6, 2H), 7.16 (t, *J*=4.1, 1H). ¹³C NMR (125 MHz,) δ 172.07, 164.79, 158.73, 140.07, 136.90, 136.12, 136.06, 133.73, 133.33, 133.30 and 126.60.

4-((4-(decyloxy) phenoxy) carbonyl) phenyl thiophene-2-carboxylate [2TWC10]

4-((thiophene-2-carbonyl)oxy)benzoic acid

(0.5 g, 2.0 mmol) and 4-decyloxy phenol (0.5 g, 2.4 mmol) were dissolved in 20 mL tetrahydrofuran (THF) solution. The solution was stirred on a magnetic stirrer, after half an hour N, N-di cyclohexyl carbodiimide (DCC) (0.6 g, 2.44 mmol) and 4-dimethylaminopyridine (DMAP) (30 mg, 0.24 mmol) dissolved in dichloromethane were added slowly. The stirring was continued for 12 hours. The reaction progress was monitored using TLC. The biproduct was filtered and the filtrate was washed with sodium bicarbonate and followed by distilled water using 250 mL separating funnel. The filtrate was evaporated to get the semi-solid. column chromatography was used to purify. Yield: 78%, colorless solid, FT-IR (KBr, cm⁻¹): 3096, 2952, 2926, 2882 (C-H stretching), 1710 (C=O), 1606 (C=C, aromatic), 1464, 1426 (C-H bending), 1278, 1145, 1094, (C-O-C). ¹H NMR (400 MHz, CDCl₃) 8.28 (d, *J*=3.8 1H), 8.21 (d, *J*=8.0, 2H), 7.62 (dd, *J*=5.0, 2H), 7.34–7.32 (m, *J*=5.0, 1H), 7.28 (d, *J*=8.0, 2H), 6.87–6.85 (d, 2H), 3.96 (t, *J*=3.4 Hz, 2H), 1.72 (p, 2H), 1.45 (m, 19H alkyl group), 1.38–1.27 (m, 4H), 0.94 (t, 2H). ¹³C NMR (100 MHz, CDCl₃) δ 164.77, 159.96, 156.99, 154.66, 144.19, 135.13, 134.03, 132.33, 131.80, 128.19, 127.39, 122.35, 121.88, 115.16, 68.48, 31.82, 29.70, 29.36, 29.28, 29.25, 26.05, 22.66, 14.10.

Synthesis of 4-bromophenyl 4-dodecyl benzoate [III]

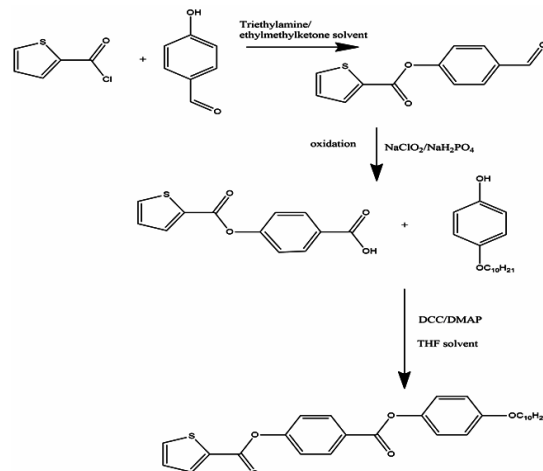
2 mL of thionyl chloride, 4-dodecylbenzoic acid (1.0 g, 3.4 mmol) and few drops of N, N-dimethyl formamide (DMF) were taken in the round bottom flask and it was refluxed for 1 h under inert atmosphere. 3 mL of triethylamine and 3 mg of DMAP were added to another flask containing 4-bromo phenol (0.58 g, 3.4 mmol) dissolved in 50 mL of dichloromethane. Then, acid chloride was added drop by drop using pressure dropping funnel at 0°C for 10 min and refluxed for 4 h at 50°C. Then the filtrate was washed using sodium bicarbonate solution. A semi solid was obtained on evaporating the solvent, column chromatography was used to purify. then, recrystallized using heptane solvent. Colorless solid was obtained. Yield: 77%, m.p.: 108-110°C. FT-IR (KBr, cm⁻¹): 2992, 2848 (C-H_{of alkylchain}), 1716 (C=O ester), 1439 (C-H bend), 1248, (C-O-C). ¹H NMR (500 MHz, CDCl₃) 8.09 (*J*=8.3, 2H, d), 7.63–7.48 (m, 2H), 7.31 (d, *J*=8.3, 2H), 7.16–7.02 (m, 2H), 2.68 (t, *J*=7.9, 2H), 1.61 (m, 2H), 1.38–1.19 (m, 19H alkyl chain), 0.88 (t, *J*=6.8, 2H). ¹³C NMR (125

MHz, CDCl_3) δ 164.98, 150.07, 149.71, 132.51, 130.30, 128.74, 126.55, 123.62, 118.88, 36.12, 31.94, 31.16, 29.68, 29.66, 29.58, 29.48, 29.38, 29.27, 22.72, 14.15.

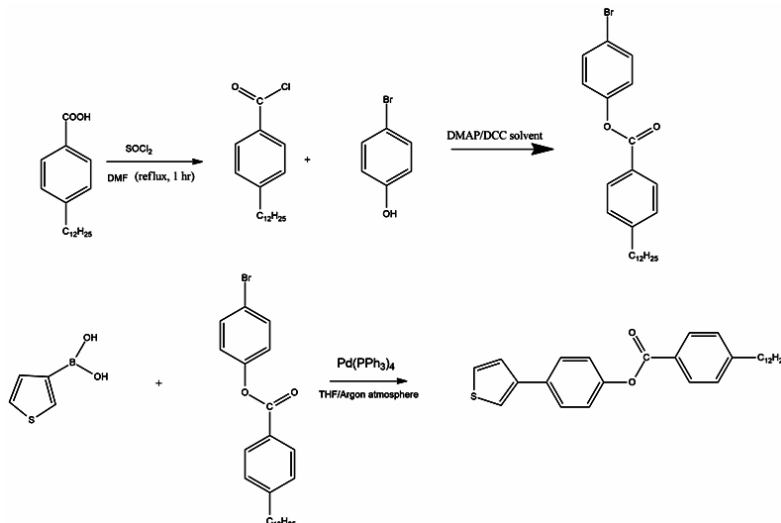
4-(Thiophen-3-yl) phenyl 4-dodecylbenzoate [S12]:

Thiophene 3-boronic acid (0.5 g, 3.9 mmol), potassium carbonate (K_2CO_3) (2.70 g, 39 mmol) and 4-bromophenyl 4-dodecyl benzoate (1.76 g, 3.9 mmol) were dissolved in 50 mL of tetrahydrofuran. Tetrakis(triphenylphosphine) palladium(0), $[\text{Pd}(\text{PPh}_3)_4]$ (92 mg, 0.3 mmol) was added to reaction mixture in the presence of argon atmosphere and the reaction was refluxed overnight at 75°C ³⁴. A semi solid was formed when the solvent was evaporated after completion of reaction. The column chromatography was used to purify impure semi solid using ethyl acetate-hexane as an eluant. Yield: 80%, colourless solid. FT-IR: 3103 (sp^2 C-H_{str}), 2981, 2940 ($-\text{CH}_2$ stretching), 1710 (C=O), 1616 (C=C), 1425, 1281, 1106 (C-O-C stretching) ^1H NMR (500 MHz, CDCl_3): δ 8.05 (d, $J=8.1$ Hz, 2H), 7.36 (m, 1H), 7.56 (d, $J=8.5$ Hz, 2H), 7.31 (m, 1H, ArH),

7.17 (d, $J=8.5$ Hz, 2H), 7.24 (m, 1H, ArH), 2.62 (t, $J=7.7$ Hz, 2H), 1.67 (p, 2H), 1.60–1.14 (m, 19H alkyl chain), 0.81 (t, $J=6.7$ Hz, 3H). ^{13}C NMR (125 MHz, CDCl_3) δ 165.30, 150.18, 149.48, 141.61, 133.67, 130.29, 128.69, 127.51, 126.94, 126.38, 126.35, 122.10, 120.38, 36.12, 31.94, 31.16, 29.68, 29.66, 29.58, 29.48, 29.37, 29.28, 22.71, 14.14.



Scheme 1. Synthesis of 2TWC10 mesogen by multistep approach



Scheme 2. Synthesis of S12 mesogen by multistep method

RESULTS AND DISCUSSIONS

FT-IR Analysis

The FT-IR spectrum of 2TWC10 and S12 mesogens were shown in Fig. 13 & 14. The comparison of both spectrums revealed that the absorption bands of Carbonyl group in both molecules were at 1710 cm^{-1} . So, there was no effect of change in terminal chain from alkoxy chain to alkyl

chain on the characteristic ester carbonyl (C=O) absorption peak. The C-O stretching frequency of S12 molecule is 1106 cm^{-1} which is due to C-O bond of ester group but for 2TWC10 the C-O absorption bands were at $1145, 1094\text{ cm}^{-1}$ which are due to ester group and alkoxy chain.

NMR analysis

The 2TWC10 molecule ^1H NMR was

shown in Fig. 1 and discussed in detail. The peaks at 8.21, 7.62, 7.28, and 6.87ppm are clearly seen as four doublets corresponding to four methine protons of core phenyl rings. For thiophene methine protons noticeably seen as multiplets at 8.28, 7.34, and 7.32ppm along with phenyl ring protons. The chemical shift values and intensity pattern of ^1H and decoupled ^{13}C NMR spectroscopy are confirming the structure of the molecule. The spectrum shows well separated 14 lines in the range of 115.16–164.77 ppm are accounted for aromatic thiophene, carbonyl carbons as well as phenyl rings. Four peaks 134.03, 122.35, 121.88, 115.16 of comparable intensity are assigned to ortho and meta carbons of the phenyl rings. The four peaks for all ortho and the meta carbons indicate rapid π -flips of the phenyl rings about their C_2 axes. three methine carbons of thiophene ring are appeared in between 135.0-128.0 ppm of moderate intensity. The low intense lines seen in the region of 164.77-134.03ppm are accounted for the quaternary carbons in the molecule.

Liquid crystalline properties by HOPM and DSC studies

The liquid crystalline property and mesophase transition enthalpies of structurally comparable molecules were investigated by polarizing optical microscope (OPM). About 2 mg of the sample was taken between glass cover slips. Only (2TWC10) exhibits typical nematic droplets further cooling gives threads texture with two or four

brushes³⁵⁻³⁷. Typically, this observation is common in three rings or four rings calamitic mesogens. The nematic phase is noticed both in heating and cooling cycle as enantiotropic manner. The appearance of nematic phase was further confirmed by DSC measurements (Fig. 6). Interestingly S12 compound does not show any liquid crystal property, it transforms from crystal to isotropic liquid in heating stage while in cooling transforms from isotropic to crystallization. The transition temperatures, mesophase type and transition enthalpy values were listed in Table 1³⁶. Typically, in DSC scan two peaks are noticed in (2TWC10) (Fig. 6). The characteristics of crystal to nematic transition has higher enthalpy value of ~ 6 kcal/ mole while for nematic to isotropic transition the enthalpy value is ~ 0.01 - 0.02 kcal/mole which are significantly lower. These results are in consistent with three or four ring rod-like mesogens reported recently. Remarkably, a close observation of optimized energy minimized structure of S12 (Fig. 12) reveals terminal alkyl chain is deviating from linearity to terminal bent shape as a result, there was a substantial decrease in the lateral dipolar interactions in the molecule. In addition, the direct linking of thiophene and phenyl ring in the molecule lead to insufficient aspect ratio of the molecule which is essential for mesophase property. So, decrease in lateral dipolar interactions due to terminal alkyl chain and insufficient aspect ratio of molecule due to direct linking of thiophene and phenyl ring in the molecule lead to absence of mesophase in S12 molecule³⁷.

Table 1: DSC data of phase transition temperatures and enthalpies of heating (ΔH in kJ/mol) and cooling cycles of thiophene mesogen. (Cr=crystalline, N=Nematic, I=Isotropic)

S. No	Compound		Melting temperature (Cr-N)	Clearing temperature (N-I)	Nematic phase stability ($^{\circ}\text{C}$)
1	2TWC10	Heating	95.5 $^{\circ}\text{C}$ (6.22)	115.5 $^{\circ}\text{C}$ (0.128)	20
		Cooling	78.2 $^{\circ}\text{C}$ (7.38)	114.1 $^{\circ}\text{C}$ (0.112)	36

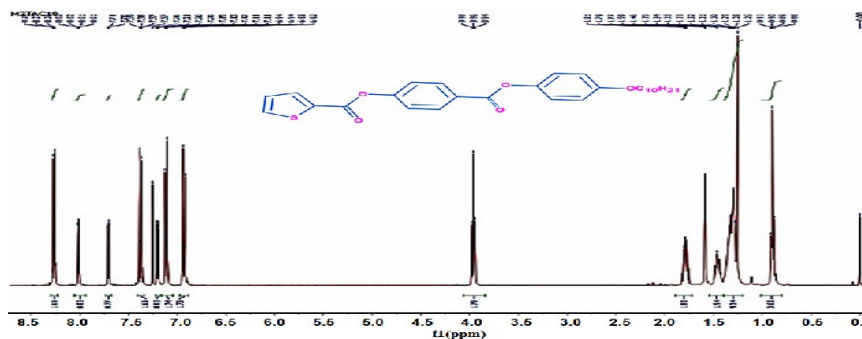
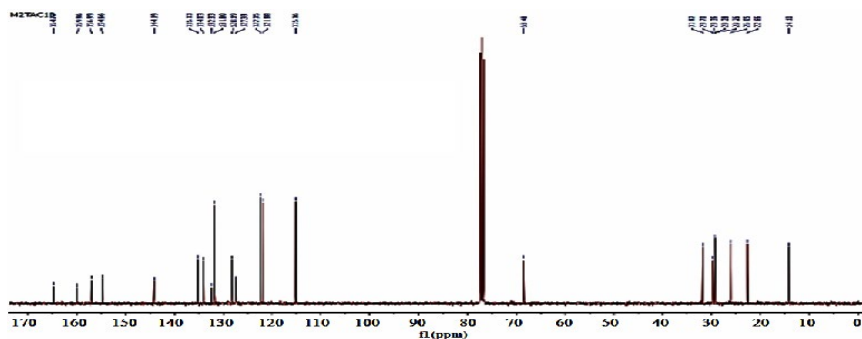
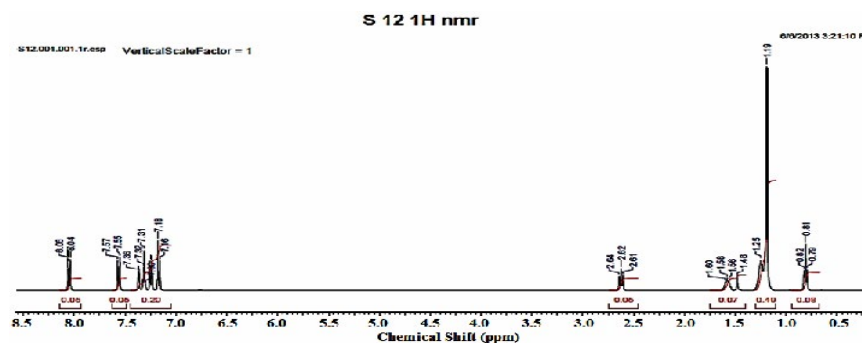
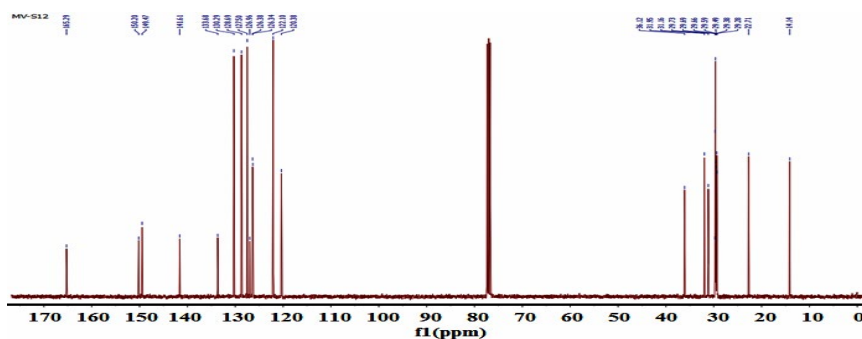


Fig. 1. Solution ^1H NMR spectrum of 2TWC10 mesogen in CDCl_3 at 25°C

Fig. 2. Solution ^{13}C NMR spectrum of 2TWC10 in CDCl_3 (25°C)Fig. 3. Solution ^1H NMR spectrum of S12 mesogen in CDCl_3 at 25°CFig. 4. Solution ^{13}C NMR spectrum of S12 mesogen in CDCl_3 at 25°C

Optical absorption in solution:

The Fig. 6,7 shows the solution UV-Visible absorption spectrum of 2TWC10 and S12 respectively. The absorption maximum of 2TWC10 was noticed around ~ 252 , $\sim 278\text{nm}$ but the absorption maximum of S12 is $\sim 300\text{nm}$, so a red shift of 20nm is observed. The 3-phenylthiophene moiety in S12 increases conjugation resulting in narrowing the energy gap of $\pi\text{-}\pi^*$ transition which lead to shift in absorption maxima towards red colour i.e., lower energy^{38,39}. This indicates a little change in structure effects the optical properties of mesogens.

Computational studies

HOMO tends to donate electron as it has

filled orbital and LUMO accepts electron as it has unoccupied orbital. The difference in energy between HOMO and LUMO is referred as band gap. The molecules having larger band gap have higher kinetic stability resulting in lower chemical reactivity (42).

Chemical reactivity

Ionization potential (IP) measures the electron donating nature which depends on the energies of highest occupied molecular orbital (HOMO). Electron affinity (EA) measures electron accepting nature which depends on energy of lowest unoccupied molecular orbital (LUMO). The ionization potential, chemical hardness, electronegativity and electron affinity

data of the two molecules are shown in Table 2. The electron affinity of alkoxy terminal 2TWC10 is lower values than alkyl terminal S12. The data of chemical reactivity descriptors like chemical potential (μ), hardness (η) was tabulated in Table 2. Chemical hardness measures the resistance to change the electron cloud density of chemical system. So, chemical hardness indicates chemical stability of the molecules. The S12 molecule has high chemical hardness,

so it is more stable than 2TWC10. Chemical potential indicates the electron-leaving tendency. The alkoxy terminal 2TWC10 has high chemical potential of -0.0719 than the chemical potential of S12 (-0.1315), so 2TWC10 is more reactive and less stable than S12, due to the high electron releasing tendency. Both the chemical reactivity descriptors i.e., chemical potential (μ), hardness (η) indicate that S12 is more stable than 2RWC10.

Table 2: Calculated Molecular properties to give insight towards the stability of molecule

Molecules	Dipole moment (Debye)	Ionization Potential (-HOMO)(au)	Electron Affinity (-LUMO)(au)	Electron negativity $\chi=1/2(I.P+E.A)$ (au)	Chemical Hardness $\eta=(I.P-E.A)$ (au)	Chemical potential $\mu=-1/2(I.P+E.A)$
S12	1.42	0.21363	0.04933	0.1315	0.1643	- 0.1315
2TWC10	2.73	0.11839	0.02546	0.0719	0.093	-0.0719

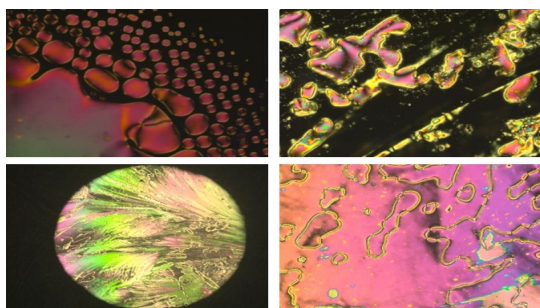


Fig. 5. HOPM photographs of nematic phase of 2TWC10

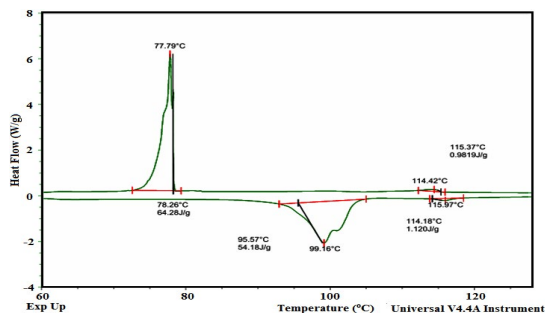


Fig. 6. DSC thermogram of 2TWC10 mesogen second heating and cooling cycles

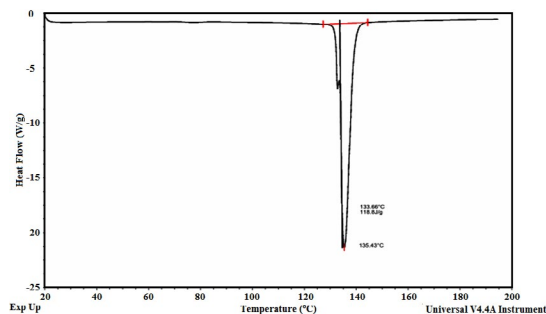


Fig. 7. DSC thermogram of S12 mesogen in first heating cycles

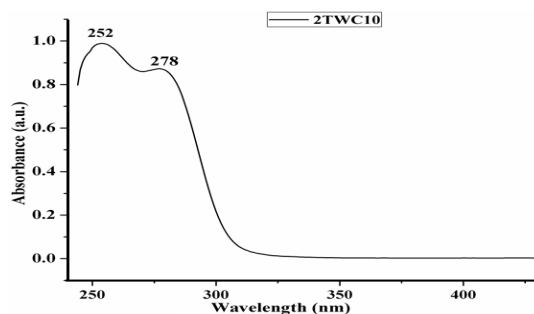


Fig. 8. 2TWC10 mesogen UV-Visible absorption spectrum in $CHCl_3$ solution at 25°C

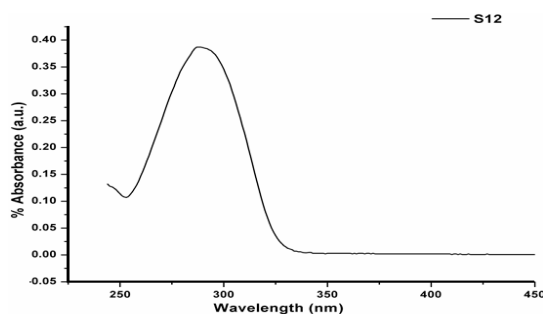


Fig. 9. S12 mesogen UV-Visible absorption spectrum in $CHCl_3$ solution at 25°C

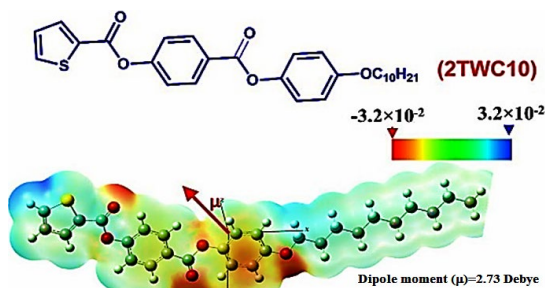


Fig. 10. MEP surface diagram of 2TWC10

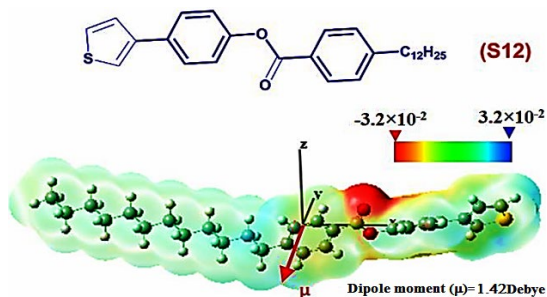


Fig. 11. MEP surface diagram of S12

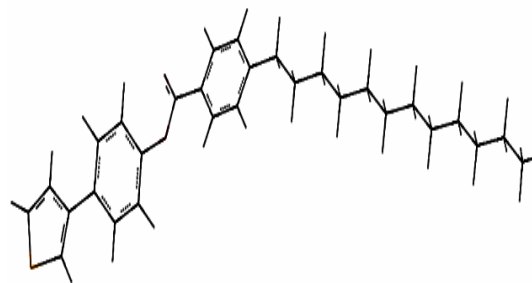


Fig. 12. DFT energy minimized structure of S12 mesogen

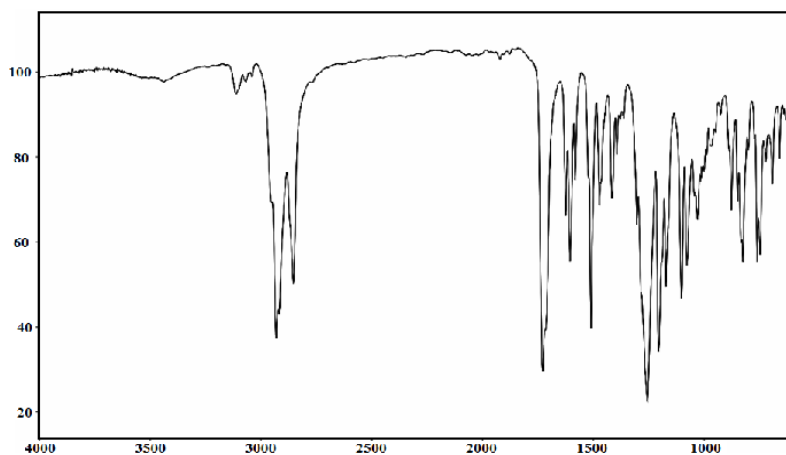


Fig. 13. FT-IR spectrum of S12 molecule

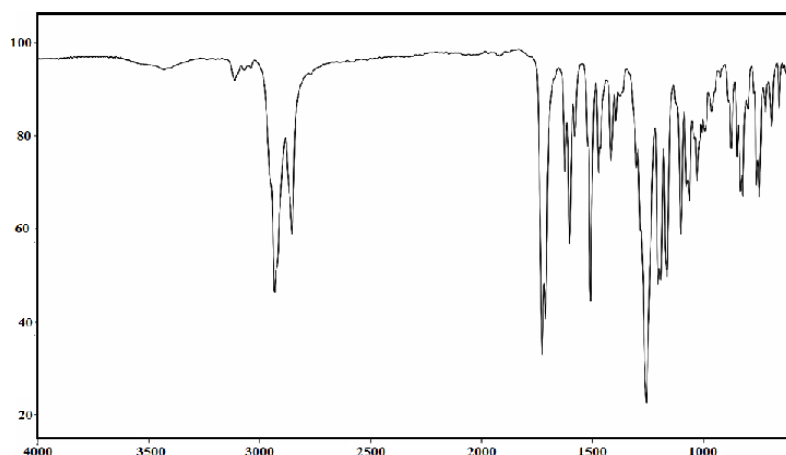


Fig. 14. FT-IR spectrum of 2TWC10

Molecular electrostatic potential (MEP) surface

The electrostatic potential map of molecules is very important tool to illustrate three-dimensional charge and electronic distribution in the molecule thereby dipole moment and polarizability of molecules. This information is helpful to predict reactive sites of the molecules where nucleophilic and electrophilic attacks occur and to study intermolecular interactions. The ESP

follows the trend blue colour > green colour > yellow colour > red colour. The blue region in the molecule has higher electrostatic potential due to low electron density so this region is prone to nucleophilic attack. The lower electrostatic potential red region has high electron density so red region in the molecule is prone to electrophilic attack (40,41). ESP (Electrostatic Potential) map of 2TWC10 and S12 high electron density on carboxylate groups

and lower electron density on thiophene ring and alkyl groups.

Dipole moment for the compounds has been calculated along the three Cartesian directions. The resultant dipole moment of 2TWC10 is higher (2.48 Debye with B3LYP/3-21G level) than S12 (1.42 Debye with B3LYP/3-21G level), the blue colour on phenyl group and its alkyl terminal in MEP surface of S12 molecule indicates uniform electron distribution in phenyl alkyl terminal chain unit. Due to uniform distribution of electrons the phenyl alkyl terminal unit is non polar. So, the overall polarity of the S12 molecule is not increased by terminal phenyl alkyl chain. The MEP surface of 2TWC10 has red region on oxygen of alkoxy terminal chain linked to phenyl ring and blue colour on remaining group indicating uneven distribution of electrons resulting in polarity of the phenyl alkoxy terminal unit, so alkoxy terminal is contributing to polarity of the molecule in 2TWC10 but in S12 there is no contribution from terminal chain to polarity due to direct linking of alkyl chain to phenyl ring.

CONCLUSION

Two thiophene based mesogens were synthesized and their mesophase properties were evaluated. The HOPM and DSC investigations revealed nematic mesophase for 2TWC10.

Remarkably, S12 does not show any liquid crystalline property. The present experimental results shows that the mesogen having terminal alkoxy chain has liquid crystal property but terminal alkyl chain mesogen do not observe any liquid crystal property. Further, differential scanning calorimetry (DSC) supported it. The UV absorption maximum of two mesogen noticed around ~252-300nm due to $\pi-\pi^*$ transition in the mesogenic core. The MEP surface diagrams are indicating that alkoxy terminal is contributing to polarity of the molecule in 2TWC10 but alkyl terminal has no contribution to the polarity of S12 molecule because the alkyl terminal group is non polar. So polarity of 2TWC10 is higher than S12 molecule. The computational studies shows that S12 molecule has high chemical hardness, so it is more stable than 2TWC10.

ACKNOWLEDGMENT

The authors are grateful to Polymer Science & Technology, CLRI, Chennai and Department of Chemistry, Sri venkateswara University, Tirupathi for their constant support and encouragement.

Conflict of Interest

No conflict of interest was reported by all the authors.

REFERENCES

1. Tschierske, C. *Isr. J. Chem.*, **2012**, *52*, 935-959.
2. Tschierske, C.; Ungar, G. *Chem Phys Chem.*, **2016**, *17*, 9-26.
3. Srinivasa, H. T.; Palakshamurthy, B. S.; Devarajegowda, H. C.; Hariprasad, S., **2018**, *1173*, 620-626.
4. Donnio, B.; Heinrich, B.; Hassan, A.; Kain, J.; Siegmar, D.; Guillon, D.; Bruce, D. W. *J. Am. Chem. Soc.*, **2004**, *126*, 15258.
5. Fang, C.; Gary, H.; Richards, J.; Kelly, S.M.; Contoret, A.E. A.; M. O'Neill., **2007**, *34*, 1249-1267.
6. Marzouk, S.; Khalfallah, A.; Heinrich, B.; KhiariKriaa, J. E. A.; Méry, S. *Journal of Fluorine Chemistry.*, **2017**, *197*, 15-23
7. Dutta, G. K.; Guha, S.; Patil, S. *Organic Electronics.*, **2010**, *11*, 1-9.
8. Yang, T.; Dai, F.; Iino, H.; Kanehara, M.; Liu, X.; Minari, T.; Liu, C.; Hanna, J., **2018**, *63*, 184-193.
9. Ahmed Jasim M.; Al-Karawi.; Ali Jasim Hammood.; Adil A.; Awad.; Al-Ameen Bariz OmarAli.; Saba Riad Khudhaier.; Dhafir T. A.; Al-Heetimi.; Samer Ghanim Majeed. *Liquid Crystals.*, **2018**, *45*(11), 16031619.
10. Ponomarenko, S. A.; Luponosov, Y. N.; Min, J.; Solodukhin, A. N.; Surin, N. M.; Shcherbin, M. A.; Chvalun, S. N.; Americ, T.; Brabec, C. *Faraday Discuss.*, **2014**, *174*, 313.
11. Sumana Y. Kotian.; Chakrabhavi Dhananjaya Mohan.; Aloir A. Merlo.; Shobith Rangappa.; Chandra Nayak, V.; Lokanatha Rai, K. M.; Kanchugarakoppal.; Rangappa, S. *Journal of Molecular Liquids.*, **2020**, *297*, 111686.
12. Ghosh, T.; Lehmann, M. *J. Mater. Chem. C.*, **2017**, *5*, 12308-12337.
13. Cai, R.; Samulski, E.T. *Liq. Cryst.*, **1991**, *9*, 617-634.

14. Dinesh Kahbtshyap.; Sunil Patel.; Varsha Prajapat.; Vinay Sharma.; Dilip Vasava, *Molecular Crystals and Liquid Crystals.*, **2019**, *681*, 58-70.
15. Santhosh Kumar Reddy, Y.; Lobo, N. P.; Sampath S.; Narasimhaswamy, T. *J. Phys. Chem. C.*, **2016**, *120*, 17960–17971.
16. Goodby, J. W.; Collings, P. J.; Kato, T.; Tschierske, C.; Gleeson, H. F.; Raynes, P. *Handbook of Liquid Crystals: Smectic and Columnar Liquid Crystals*, Wiley-VCH, Weinheim, Germany, **2014**, *4*, 3–41.
17. Akagi, K.; Perepichka, Ed. I. F.; Perepichka, Hand Book of Thiophene-Based Materials: Applications in Organic Electronics and Photonics. John Wiley and Sons: Chichester, UK., **2009**.
18. Li, Y.-X., Fan, F.-F., Wang, J., Cseh, L., Xue, M., Zeng, X.-B., and Ungar, G. *Chem. Eur. J.*, **2019**, 02639.
19. Sivaraman, P.; Thakur, P. A.; Shashidhara, K. *Synthetic Metals.*, **2020**, *259*, 116255.
20. Nunes da Silva, F.; Santos da Silva, A.; Bechtold, I. H.; Eduardo Zap, André Alexandre Vieira. *Liquid Crystals.*, **2019**, *46*(11), 1707-1717.
21. Kakekochi, V.; Nikhil, P.; Chandrasekharan, K.; Udaya Kumar, D. *Dyes and Pigments.*, **2020**.
22. Pankaj Kumar, C.; Vandna Sharma, Praveen Malik.; Raina, K.K. *Journal of Molecular Structure.*, **2019**, *1196*, 866-873.
23. Fall, W. S.; Yen, M.-H.; Zeng, X.; Cseh, L.; Liu, Y.; Gehring, G.; Ungar, G. *Soft Matter.*, **2019**, *15*, 22-29.
24. Moriguchi, T.; Higashi, M.; Yakeya, D.; Venkataprasad, J.; Akihiko, T.; Okauchi, T.; Nagamatsu, S.; Takashima, W. *J. Mol. Str.*, **2017**, *1127*, 413-418.
25. Kim, S.; Kim, A.; Jang, K.S.; Yoo, S.; Ka, J.W.; Kim, J.; Yi, M.H.; Won, J.C.; Hong, S.K.; Kim, Y.H. *Synth. Met.*, **2016**, *220*, 311–317.
26. Kato, T. Uchida, J.; Ichikawa, T.; Sakamoto, T. *Angew. Chem. Int. Ed.*, **2018**, *57*, 4355–4371.
27. Giroto, E.; Eccher, J.; Vieira, A.A.; Bechtold, I.H.; Gallardo, H. *Tetrahedron.*, **2014**, *70*, 3355-3360.
28. Yuki Arakawa, Kenta Komatsu, Satoyoshi Inui, Hideto Tsuji. *J. of Mole. Str.*, **2020**, *1199*, 126913.
29. Ester, D. F.; McKearney, D.; Herasymchuk K.; Vance E. Williams, *Materials.*, **2019**, *12*(14), 2314.
30. Becke, D.; *J. Chem. Phys.*, **1993**, *98*, 5648.
31. Liegault, B.; Lapointe, D.; Caron, L.; Vlassova, A. and Fagnou, K. *J. Org. Chem.*, **2009**, *74*, 1826.
32. Rajasekhar Reddy, K.; Varathan, E.; Lobo, N. P.; Easwaramoorthi, S.; Narasimhaswamy, T. *J. Phys. Chem. C.*, **2016**, *120*, 2257.
33. Greene, W. *Protecting Groups in Organic Synthesis*; John Wiley & Sons: New York., **1999**.
34. Benalloua, S.; Besbesa, S.S.; Greletb, E.; Bentaleb, A. *Mol. Cryst. Liq. Cryst.*, **2017**, *647*, 290-298.
35. Kelker, H.; Hatz, R. *Hand Book of Liquid Crystals*; Verlag Chemie: Weinheim., **1980**.
36. Luckhurst, G. R.; Gray, G. W. *The Molecular Physics of Liquid Crystals*; Academic Press: New York., **1979**.
37. Ananthakrishnan, S. J.; Prakash Wadgaonkar, P.; Somanathan, N.; *Phys. Chem. Chem. Phys.*, **2014**, *16*, 23809-23818.
38. Belletete, M.; Mazerolle, L.; Desrosiers, M.; Leclerc, M.; Durocher, G. *Macromolecules.*, **1995**, *28*, 8587-8597.
39. F. Andreani, L. Angiolini, V. Greci, E. Salatelli, *Synthetic Metals.*, **2004**, *145*, 21-227.
40. Srinivasu, K.; Ghosh, S.K.; Das, R.; *RSC Adv.*, **2012**, *2*, 2914–2922.
41. Chattaraj, P. K.; Maiti, B.; Sarkar, U. *J Phys Chem A.*, **2003**, *107*, 4973–4975.
42. Ghara, M.; Pan, S.; Deb, J.; *J Chem Sci.*, **2016**, *10*, 1537–1548.